Steel and Composite Structures, Vol. 9, No. 1 (2009) 19-38
DOI: http://dx.doi.org/10.12989/scs.2009.9.1.019

Recycled aggregate concrete filled steel SHS beam-columns subjected to cyclic loading

You-Fu Yang*

State Key Laboratory of Coastal and Offshore Engineering, Dalian University of Technology, Dalian, 116024, China

Lin-Tao Zhu

College of Civil Engineering, Fuzhou University, Fuzhou, 350002, China

(Received October 8, 2007, Accepted January 2, 2009)

Abstract: The present paper provides test data to evaluate the seismic performance of recycled aggregate concrete (RAC) filled steel square hollow section (SHS) beam-columns. Fifteen specimens, including 12 RAC filled steel tubular (RACFST) columns and 3 reference conventional concrete filled steel tubular (CFST) columns, were tested under reversed cyclic flexural loading while subjected to constant axially compressive load. The test parameters include: (1) axial load level (n), from 0.05 to 0.47; and (2) recycled coarse aggregate replacement ratio (r), from 0 to 50%. It was found that, generally, the seismic performance of RACFST columns was similar to that of the reference conventional CFST columns, and RACFST columns exhibited high levels of bearing capacity and ductility. Comparisons are made with predicted RACFST beam-column bearing capacities and flexural stiffness using current design codes. A theoretical model for conventional CFST beam-columns is employed in this paper for square RACFST beam-columns. The predicted load versus deformation hysteretic curves are found to exhibit satisfactory agreement with test results.

Keywords: recycled aggregate concrete filled steel tube (RACFST); recycled aggregate concrete (RAC); composite columns; cyclic loads; capacity; flexural stiffness; ductility.

1. Introduction

Recycling demolished concrete as new aggregates for the production of concrete in construction is not fresh and the summary of the relevant literature has been available (Hansen 1992, Rao *et al*. 2007). Prior studies carried out on recycled aggregate concrete (RAC) showed that, generally, due to the lower strength and elastic modulus, weaker workability and freeze-thaw resistance, and higher shrinkage and creep of RAC compared with conventional concrete with natural aggregates (Rao *et al*. 2007, Ajdukiewicz and Kliszczewicz 2002), RAC was mainly used in lower level applications, such as general bulk fill material, base or fill in drainage projects, sub-base or surface material in road construction, and so forth (Etxeberria *et al*. 2007). However, RAC was well appreciated because of its better abrasion resistance, better performance exposed to high temperatures, lower brittleness as well as the lower specific gravity that reduce the self-weight of the structures (Evangelista and de Brito 2007, Zega and Di Maio 2006).

* Corresponding Author, Email: youfuyang@163.com

Most importantly, large-scale recycling of demolished concrete will contribute not only to the solution of a growing waste storage problem, but also to the conserving of limited natural resources of sand and stone and the reduction of transport costs (Hansen 1992, Poon and Chan 2007).

In the past, many studies were performed to investigate the properties of recycled aggregates and RACs, and several design methods had been established in different countries or regions (Hansen 1992, Etxeberria *et al*. 2007). However, only few researches were carried out on the seismic behaviour of RAC structures subjected to cyclic forces, and Yang *et al*. (2008) had presented a brief review on these works.

Tests on seismic performance of RAC filled circular steel tubular beam-column had been carried out by the authors. In previous studies (Yang *et al*. 2008), thirteen composite specimens with circular section, including 10 RAC filled steel tubular (RACFST) columns and 3 reference conventional concrete filled steel tubular (CFST) columns, were tested under constant axial load and cyclically increasing flexural loading. Moreover, Yang and Han (2006a, 2006b) also studied the performance of RACFST stub columns, beams and slender columns subjected to short-term static loading.

The present study is an attempt to investigate the seismic performance of RAC filled steel square hollow section (SHS) columns under reversed cyclic flexural loading while subjected to constant axially compressive load. The main objectives of this research are fourfold: first, to report a series of new tests on composite beam-columns; second, to analyze the effect of several parameters on the seismic performance of RACFST beam-columns; third, to compare the predicted member capacity and flexural stiffness by using current design codes; and finally, to predict the load versus deformation hysteretic relations with a theoretical model.

2 Experimental Programs

2.1. Test specimen

Fifteen specimens with square section, including 12 recycled aggregate concrete (RAC) filled steel tubular (RACFST) beam-columns and 3 reference conventional concrete filled steel tubular (CFST) beam-columns, were tested under reversed cyclic flexural loading while subjected to constant axially compressive load. Fig. 1 shows the cross section of the tested specimens, where, B is the overall face width of square steel tube; t is the wall thickness of steel tube; and r_i is the internal corner radius. The test parameters are the axial load level and recycled coarse aggregate (RCA) replacement ratio.

The axial load level (n) is defined as following, i.e.

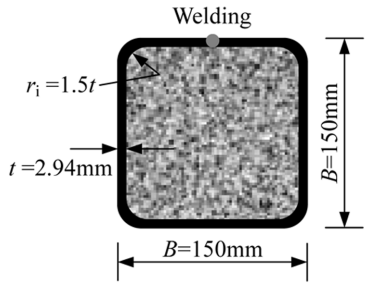

Fig. 1 Cross-sectional dimension of the test specimens

$$n = \frac{N_o}{N_u} \tag{1}$$

where, N_o is the axially compressive load applied on the composite columns; N_u is the axially compressive capacity of the composite columns, and can be determined by using theoretical model described by Yang and Han (2006b). Concrete strength at the time of the test was used in the calculation.

The recycled coarse aggregate (RCA) replacement ratio (r) in this paper is defined as the percentage of RCA within the whole coarse aggregate by weight.

The detail information of the tested specimens is listed in Table 1. The labels used to depict each specimen are as follows:

- Axial load level [L : low (n = 0.05), M : middle (n = 0.25), H : high (n = 0.43 and 0.47)];
- RCA replacement ratio [A : r = 0 (conventional concrete), B : r = 25%, C : r = 50%).

For example, the specimen beginning with the label "MB-2" denotes the second specimen with r of 25%, and its axial load level is 0.25.

The ends of the tubes were cut and machined to the required length and the insides of the tubes were wire brushed to remove any rust and loose debris present. The deposits of grease and oil, if any, were cleaned away. Each tube was welded to a square steel base plate 16 mm thick. The concrete was filled in layers and was vibrated by poker vibrator. The specimens were placed upright to air-cure at room temperature until testing.

2.2. Material properties

The tubes were all cut from long cold-formed steel SHS. Standard tensile coupon tests were carried

Table 1 Specimen information and test results

No.	Specimen label	$B \times t$ (mm)	B/t	f_{cu} (MPa)	N_o (kN)	n	P_{ue} (kN)	P_{ua} (kN)	P_{ua}/P_{ue}	K_{ie} (kN.m^2)	K_{se} (kN.m^2)	DI
1	LA	□-150 × 2.94	51	60.4	69.9	0.05	109.8	110.6	1.007	1896	1428	7.96
2	LB-1	□-150 × 2.94	51	59.2	69.1	0.05	106.9	107.5	1.006	1748	1425	8.68
3	LB-2	□-150 × 2.94	51	59.2	69.1	0.05	106.1	107.5	1.013	1784	1380	8.96
4	LC-1	□-150 × 2.94	51	52.2	64.3	0.05	105.3	106.9	1.015	1663	1368	9.41
5	LC-2	□-150 × 2.94	51	52.2	64.3	0.05	105.4	106.9	1.014	1733	1339	9.36
6	MA	□-150 × 2.94	51	60.4	349.7	0.25	124.5	118.5	0.952	1969	1729	4.87
7	MB-1	□-150 × 2.94	51	59.2	345.7	0.25	122.8	117.7	0.958	1956	1636	5.47
8	MB-2	□-150 × 2.94	51	59.2	345.7	0.25	122.9	117.7	0.958	1923	1715	5.28
9	MC-1	□-150 × 2.94	51	52.2	321.4	0.25	119.3	114.5	0.960	1864	1709	5.94
10	MC-2	□-150 × 2.94	51	52.2	321.4	0.25	119.1	114.5	0.961	1877	1585	6.01
11	HA	□-150 × 2.94	51	60.4	600	0.43	133.1	118.1	0.887	2109	1785	3.29
12	HB-1	□-150 × 2.94	51	59.2	600	0.43	129.8	117.2	0.903	2073	1721	3.32
13	HB-2	□-150 × 2.94	51	59.2	600	0.43	129.3	117.2	0.906	2048	1733	3.49
14	HC-1	□-150 × 2.94	51	52.2	600	0.47	127.6	107.2	0.840	2031	1729	3.99
15	HC-2	□-150 × 2.94	51	52.2	600	0.47	127.2	107.2	0.843	2072	1561	3.71

out to measure material properties of the steel tube. Three coupons were cut from the flat portion of the tube. The yield strength was obtained from the 0.2% offset method. From these tests, the average yield strength, tensile strength and modulus of elasticity were found to be 344.4 MPa, 450.5 MPa and 207,000 MPa, respectively. The Poisson's ratio of the steel was 0.292.

Two types of recycled aggregate concrete (RAC) with RCA replacement ratio (r) of 25% and 50%, and the reference conventional concrete were prepared. The mix was designed for a 28-day compressive cube strength (f_{cu}) of approximately 40 MPa. The RCA was gotten by crushing waste concrete (self-consolidating concrete) in the failure conventional CFST specimens. The natural coarse aggregate (NCA) and RCA were sieved with a mesh square of 26.5 mm, and both of them had the similar sieve grading, i.e. 5~16 mm coarse aggregates are about 55% in weight and 16~26.5 mm coarse aggregates are about 45% in weight. The mix proportions of the waste concrete were as following: Cement: 300 kg/m^3; Fly ash: 200 kg/m^3; Natural fine aggregate: 994 kg/m^3; Natural coarse aggregate: 720 kg/m^3; Water: 181 kg/m^3 and High range water reducer: 5 kg/m^3; and its 28-day compressive cube strength and elastic modulus were 52.6 MPa and 41464 MPa, respectively. The mix proportions and properties of new concrete were listed in Table 2. In all the concrete mixes, the fine aggregate used was siliceous sand, and the NCA was carbonate stone, which was the same as that used in the waste concrete. The workability of new concrete was also presented in Table 2. It is shown that, the slump value of the mixture decreased with the increase of RCA replacement ratio (r). Although the slump value of RAC is lower than that of the reference conventional concrete, there is no difficulty in obtaining the desired uniformity and subsequent compactness of RAC.

The test specimens were cast from three batches of concrete. Several 150 mm cubes and 150 mm × 300 mm prisms were also cast for each type of concrete, and cured in conditions similar to the corresponding composite columns.

2.3. Test Setup and procedure

The specimens were tested under reversed cyclic flexural loading while subjected to constant axially compressive load. The length of the test specimens is 1500 mm. The comprehensive descriptions of the test setup can be found in Han and Yang (2005), Han *et al*. (2003, 2005a, 2005b, 2006). Fig. 2 is a general view of the test setup. The axial load (N_o) was applied and kept constant by a 1000 kN hydraulic ram. The flexural loading was applied by imposing cyclically lateral forces in the middle section of the specimen via a MTS hydraulic ram with 250 kN capacity. Displacement transducers (DTs) and curvature gauges were used to measure the in-plane deflections and bending curvatures of the test specimens. The lateral loading history, which was described in detail by Yang *et al*. (2008) and Han *et al*. (2005a, 2005b,

Table 2 Mix proportions and properties of new concrete

Type of concrete	Cement (kg/m^3)	Sand (kg/m^3)	NCA (kg/m^3)	RCA (kg/m^3)	Water (kg/m^3)	W/C	28-day cube strength, f_{cu} (MPa)	Test-day cube strength, f_{cu} (MPa)	Modulus of elasticity, E_c (MPa)	Slump (mm)
Conventional concrete	414	630	1170	0 (r = 0)	207	0.5	42.7	60.4	2.75×10^4	40
Recycled aggregate concrete	414	630	878	292 (r = 25%)	207	0.5	41.8	59.2	2.61×10^4	35
	414	630	585	585 (r = 50%)	207	0.5	36.6	52.2	2.46×10^4	33

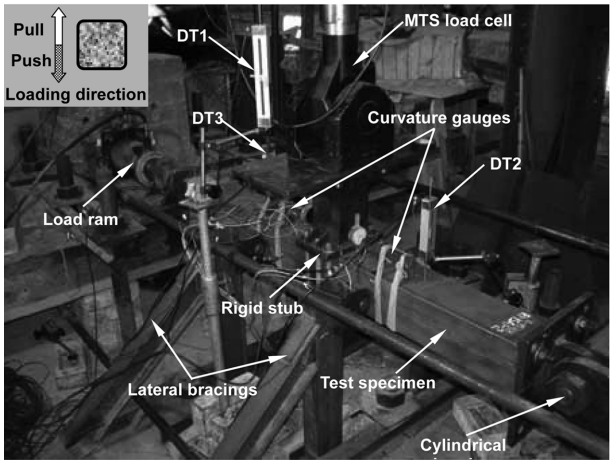

Fig. 2 A general view of the test setup

2006), was generally based on ATC-24 guidelines (1992) for cyclic testing of structural steel components.

The test was conducted until either the specimen failed due to fracture of the steel tube or the specimen lateral force resistance had deteriorated to 50% of the lateral bearing capacity. Each load interval was maintained for 2 minutes. No deformations at the reaction blocks were observed until the column bowed after reaching the failure load.

3 Test results and discussions

3.1. General behaviours

From the tests, it was found that all specimens had relatively good ductility and post-peak bearing capacity and the test progressed in a smooth and controlled fashion. The performance of RACFST specimens was similar to that of the reference conventional CFST specimens. The lateral bearing capacities (P_{ue}) were noted by the global buckling and subsequent bending of the specimens. In general, after the deflection reached yield level lateral deflection (δ_y), an outward indent or bulge firstly formed close to the rigid stub at the initial compression flange of steel SHS on both sides of the rigid stub. The bulge also formed on the other flange of steel SHS when the lateral force was reversed. When two times of δ_y were obtained, the range of buckle became big and gradually extended to whole cross section except for the corner region. When the specimen approached failure, the bugle nearly formed a complete ring on each side of the stub, and gray white small cracks were produced at the corner part of the steel tube, due to its higher residual stress and lower plasticity compared with the flat portion. At the end of the test, the steel tube fractured at the location of the corner part with small cracks. It was found that, the failure features of the RACFST specimens after subjected to cyclic loadings were similar to those of steel tube confined concrete (STCC) columns, self-consolidating concrete (SCC) filled hollow structural steel (HSS) columns, and concrete filled double-skin steel tubular (CFDST) columns (Han *et al*. 2005a, 2005b, 2006).

Figs. 3 and 4 show the typical failure mode of the RACFST specimens and reference conventional CFST specimen; and their core concrete after the test and removing the middle rigid stub, respectively. It can be seen that, generally, for the tested specimens, the buckle of steel tube is produced near the rigid

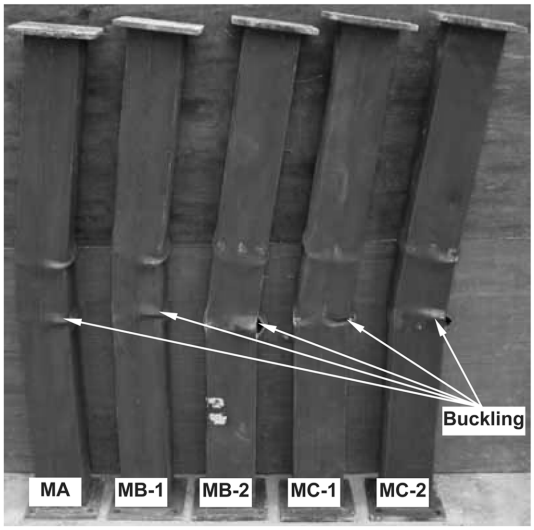

Fig. 3 Typical failure modes of the tested specimens

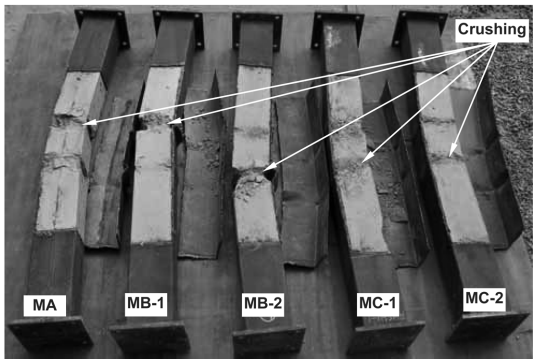

Fig. 4 Typical failure modes of the core concrete

stub, without reference to the RCA replacement ratio (r) and axial load level (n). This may be explained that, just as the core concrete in conventional CFST, the outer steel SHS can provide good confinement and thus improve the characteristics of core RAC in RACFST. So the failure mode of RACFST specimens is not obviously different from that of the reference conventional CFST specimens. The failure mode of core concrete is the crushing at local buckling site of the steel tube.

The measured lateral force (P) versus the mid-span lateral deflection (δ) curves of all tested specimens are shown in Fig. 5, where '○' and '□' denote the starting of yield and fracture of the steel tube, respectively. It can be found that, when the axial load level is same or similar, no obvious discrepancy in the shape of $P-\delta$ curves is found between RACFST beam-columns and the reference conventional CFST beam-columns. The maximum lateral forces (P_{ue}) obtained in the test are presented in Table 1, where P_{ue} is the average value of the bearing capacities in two loading directions.

The test results showed that, for all tested specimens, the lateral deflection curves in two loading directions were approximately in the shape of a half-sine wave. Fig. 6 illustrates the lateral deflection development of specimen MB-1 with different force levels (P) before and after reaching the bearing

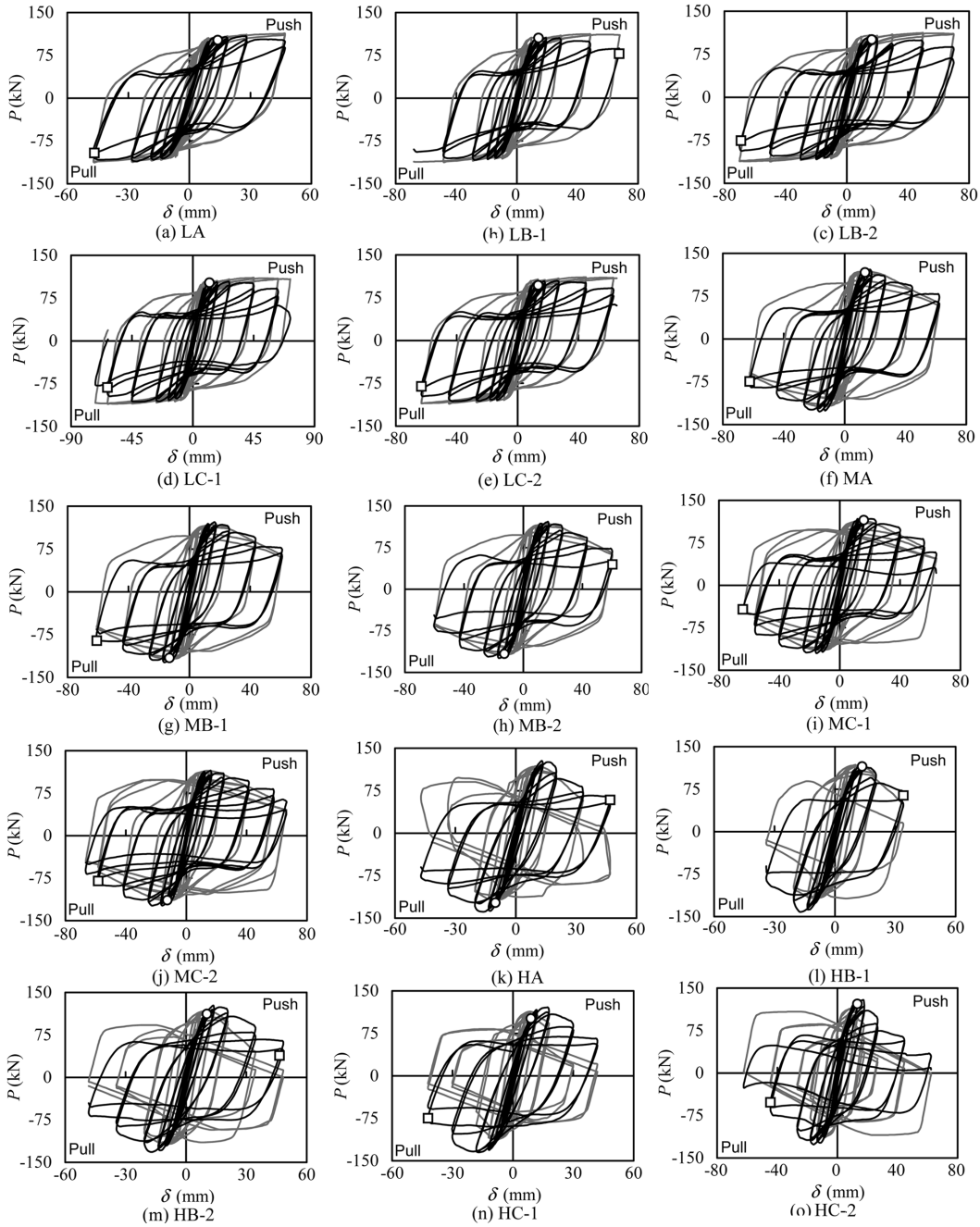

Fig. 5 Lateral force (P) versus mid-span lateral deflection (δ) curves (—— Measured curve; —— Predicted curve) (○ Steel tube yieding point; □ Steel tube fracture point)

capacity, where p equals to P/P_{ue}. In Fig. 6, the dashed lines are the sinusoids with the same deflections in the mid-span.

It was found that the curvature readings from the two curvature gauges mounted on the specimens

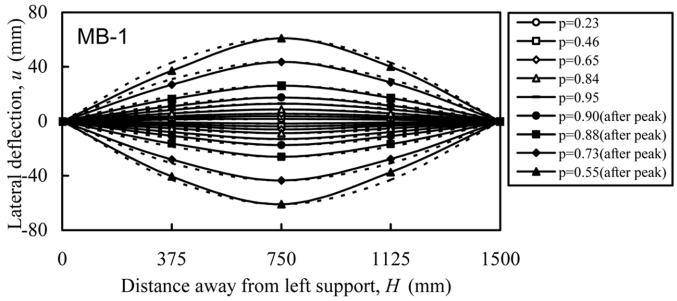

Fig. 6 Length versus lateral deflection curve of a typical specimen (—— Measured curve - - - - - Half-sine wave)

around the stub rigid (see Fig. 2) were practically the same for all tested specimens. Just like P-δ relationships, there was no evident difference in the shape of moment (M) versus curvature (ϕ) curves between RACFST specimens and the reference conventional CFST specimens when the axial load level was same or similar. Specimen MB-1 is chosen to indicate the typical M-ϕ response, as shown in Fig. 7. The M-ϕ graphs show that, there is an initial elastic response, then inelastic character with gradually decreasing stiffness, until achieving the ultimate moment (M_{ue}) asymptotically. The test results indicate that, generally, M-ϕ curve goes into the inelastic stage at 20% of M_{ue}, so the initial section flexural stiffness (K_i) is defined as the secant stiffness corresponding to a moment of $0.2M_{ue}$. The M-ϕ response is also used to determine the serviceability-level section flexural stiffness (K_s), which is defined as the secant stiffness corresponding to the serviceability-level moment of 0.6 M_{ue} (Varma *et al*. 2002). The tested initial section flexural stiffness (K_{ie}) and serviceability-level section flexural stiffness (K_{se}) are also presented in Table 1, where K_{ie} and K_{se} are the average value of the measured initial and serviceability-level section flexural stiffness in two loading directions.

3.2. Effects of axial load level

Figs. 8 and 9 illustrate the effect of axial load level (n) on typical $P/P_{ue} - \delta$ envelope curves, as well as

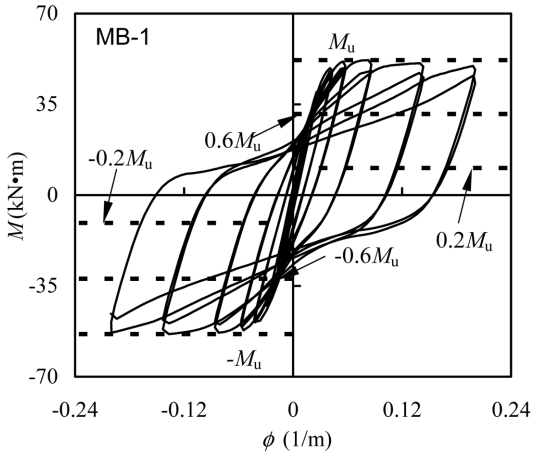

Fig. 7 Moment (M) versus curvature (ϕ) relation of a typical specimen

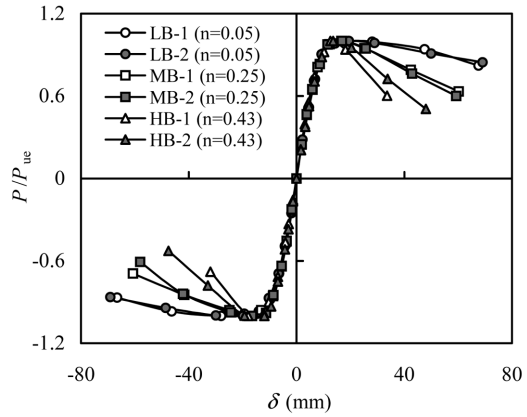

Fig. 8 Effect of n on typical $P / P_{ue} - \delta$ envelope curves of RACFST columns ($r = 25\%$)

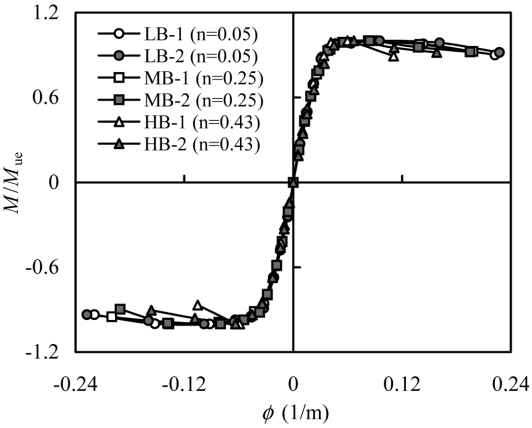

Fig. 9 Effect of n on typical $M / M_{ue} - \phi$ envelope curves of RACFST columns ($r = 25\%$)

$M / M_{ue} - \phi$ envelope curves of the tested specimens, respectively. It is shown that, the axial load level (n) has an obvious effect on the ductility of the specimen; and in general, the ductility decreases with the increase of the axial load level. This may be explained that, at the post-peak stage, the higher damage of concrete core was caused by the higher axial load level.

The effects of axial load level (n) on the measured lateral bearing capacities (P_{ue}) of the tested specimens are shown in Fig. 10. It can be seen that, within the limitations of the current tested specimens, the bearing capacities increase with the increase of axial load level irrespective of the RCA replacement ratio. This may be due to the fact that, when the axial load level is relatively small (up to 0.47 in the current test), the higher the axial load level, the bigger the contribution of core concrete to the bearing capacity and the higher the longitudinal restriction of the axially compressive load. The similar phenomena were found in previous tests on composite beam-columns with circular section (Yang *et al*. 2008).

The effects of axial load level (n) on the initial section flexural stiffness (K_{ie}) and serviceability-level flexural stiffness (K_{se}) of the tested specimens are illustrated in Fig. 11. Generally, the increased initial and serviceability-level section flexural stiffness is produced for the specimens with relatively high

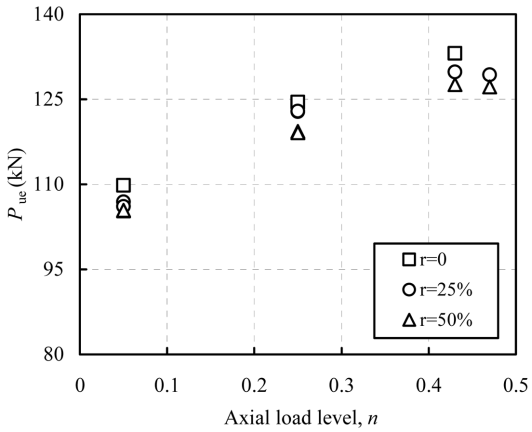

Fig. 10 Effects of n and r on P_{ue}

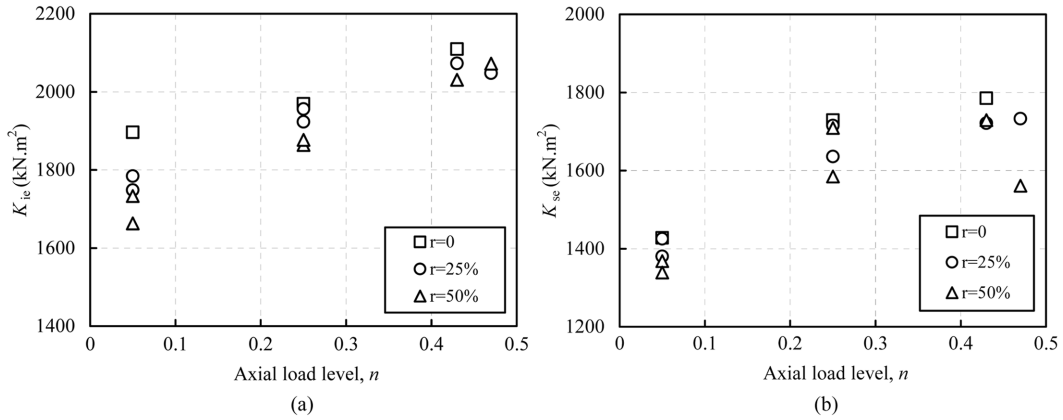

Fig. 11 Effects of n and r on K_{ie} and K_{se}

axial load level, without reference to the RCA replacement ratio (r). This may be due to the fact that, the higher axial load level results in bigger compression area of core concrete, which improves the contribution of core concrete to the stiffness.

Fig. 12 shows the total dissipated energy (E) in each cycle, where E is obtained from the lateral force (P) versus lateral deflection (δ) curve as the area bound by the hysteretic loop of that cycle (Han *et al*. 2006). It can be seen that, at the same lateral deflection ratio (δ/δ_y), the specimens with higher axial load level result in lower total dissipated energy due to its lower ductility and higher damage of concrete core after achieving the bearing capacity.

In order to quantify the ductility of RACFST columns and the reference conventional CFST columns under reversed cyclic flexural loading while subjected to constant axially compressive load, the ductility index (DI) is defined as following (Yang *et al*. 2008, Han and Yang 2005):

$$DI = \frac{\delta_u}{\delta_y} \tag{2}$$

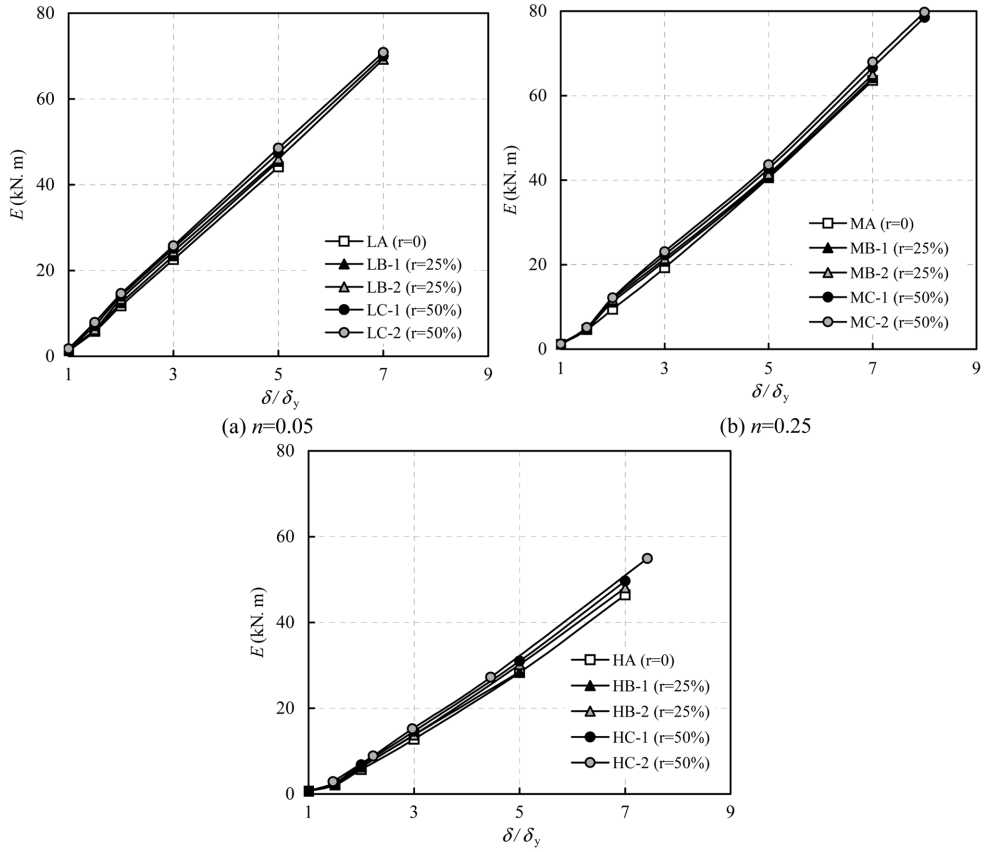

(a) n=0.05 (b) n=0.25

(c) n=0.43 and 0.47

Fig. 12 Dissipation ability

where, δ_y is the yield lateral deflection, δ_u is the lateral deflection when the lateral force falls to 85% of the bearing capacity (P_{ue}) in P - δ envelope curve.

The *DI* values so determined are summarized in Table 1, where *DI* is the average value in two loading directions. For the specimens with low axial load level (e.g. n = 0.05), as the descending portion of $P-\delta$ envelope curve does not fall below $0.85P_{ue}$, the maximum mid-span deflection is assumed to be δ_u to obtain the ductility index (*DI*). Fig. 13 shows the effects of axial load level (n) on the ductility index (*DI*). It can be found that, the higher the axial load level, the lower the ductility index is, irrespective of the RCA replacement ratio.

3.3. Effects of RCA replacement ratio

The effects of RCA replacement ratio on typical $P/P_{ue}-\delta$ and $M/M_{ue}-\phi$ envelope curves are shown in Figs. 14 and 15, respectively. It can be found from these figures that, in general, the RCA replacement ratio has moderate influences on the shape of the envelope curves; however, RACFST specimens show slightly higher ductility than the reference conventional CFST specimens.

To account for the influences of RCA replacement ratio (r) on the lateral bearing capacities of the

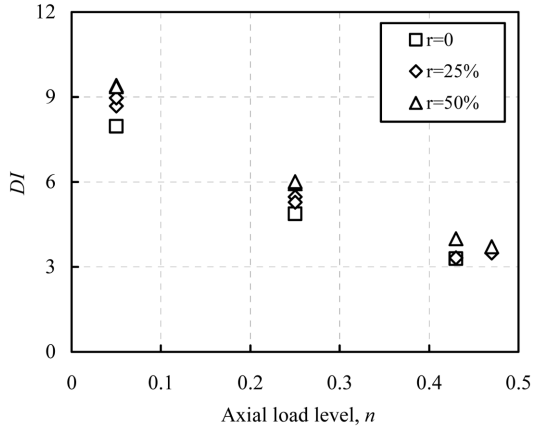

Fig. 13 Effects of n and r on DI

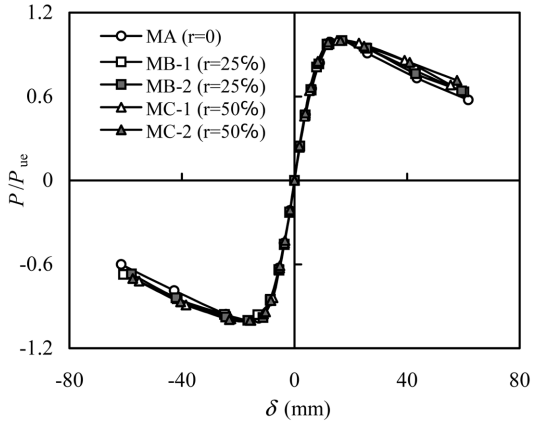

Fig. 14 Effect of r on typical $P / P_{ue} - \delta$ envelope curves ($n = 0.25$)

tested specimens, the loss of capacity index (CI) is defined. It is expressed as:

$$CI = \frac{P_{ue,A} - P_{ue,B}(or \ \ P_{ue,C})}{P_{ue,A}} \tag{3}$$

where, $P_{ue,A}$ is the bearing capacity of the specimens with conventional concrete; $P_{ue,B}$ and $P_{ue,C}$ are the bearing capacity of the specimens with r of 25% and 50%, respectively.

The loss of capacity indexes (CI) so determined are summarized in Table 3. In the calculations, $P_{ue,B}$ and $P_{ue,C}$ are taken as the average value of two same specimens.

It can be found from Table 3 that, generally, the columns with conventional concrete generated slightly higher bearing capacities (P_{ue}) over RACFST columns with r of 25% and 50% by 1.3% to 3%, and 4.1% to 4.3%, respectively. In terms of lateral bearing capacity compared with the reference conventional CFST columns, the performance of RACFST columns is expected to be comparable, as only 1.3% to 4.3% bearing capacity decreases are induced in RACFST columns. This may be due to the

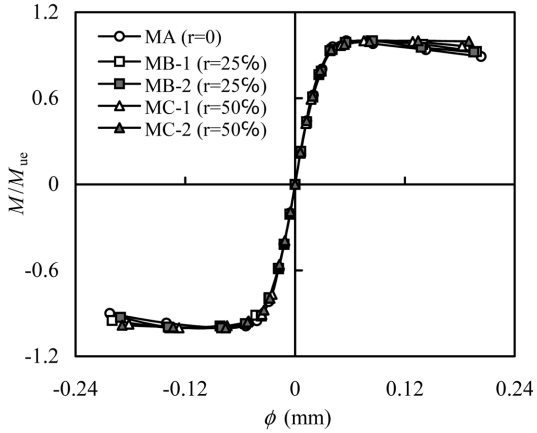

Fig. 15 Effect of r on typical $M / M_{ue} - \phi$ envelope curves ($n = 0.25$)

Table 3 Comparisons between RACFST columns and normal CFST columns

No.	Specimen label	P_{ue} (kN)		K_{ie} (kN.m^2)		K_{se} (kN.m^2)		CI	SI_i	SI_s
		Measured value	Average value	Measured value	Average value	Measured value	Average value			
1	LA	109.8	109.8	1896	1896	1428	1428	-	-	-
2	LB-1	106.9	106.5	1748	1766	1425	1402.5	3%	6.9%	1.8%
3	LB-2	106.1		1784		1380				
4	LC-1	105.3	105.35	1743	1738	1368	1353.5	4.1%	8.3%	5.2%
5	LC-2	105.4		1733		1339				
6	MA	124.5	124.5	1969	1969	1729	1729	-	-	-
7	MB-1	122.8	122.85	1956	1939.5	1636	1675.5	1.3%	1.5%	3.1%
8	MB-2	122.9		1923		1715				
9	MC-1	119.3	119.2	1864	1870.5	1709	1647	4.3%	5%	4.7%
10	MC-2	119.1		1877		1585				
11	HA	133.1	133.1	2109	2109	1785	1785	-	-	-
12	HB-1	129.8	129.55	2073	2060.5	1701	1712	2.7%	2.3%	4.1%
13	HB-2	129.3		2048		1723				
14	HC-1	127.6	127.4	2031	2051.5	1729	1645	4.3%	2.7%	7.8%
15	HC-2	127.2		2072		1561				

fact that, at the test day, the compressive cube strength of RAC with 25% and 50% RCA is 2% and 13.6% lower than that of the control conventional concrete, respectively.

For convenience of evaluating the influences of RCA replacement ratio (r) on the section flexural stiffness of the tested specimens, the loss of initial section flexural stiffness index (SI_i) and serviceability-level section flexural stiffness index (SI_s) are defined as follows:

$$SI_i = \frac{K_{ie,A} - K_{ie,B}(or\ \ K_{ie,C})}{K_{ie,A}} \tag{4}$$

$$SI_s = \frac{K_{se,A} - K_{se,B}(or\ K_{se,C})}{K_{se,A}} \quad (5)$$

where, $K_{ie,A}$ and $K_{se,A}$ are the initial section flexural stiffness and serviceability-level section flexural stiffness of the specimens with conventional concrete; and $K_{ie,B}(K_{se,B})$ and $K_{ie,C}(K_{se,C})$ are the initial section flexural stiffness (serviceability-level section flexural stiffness) of the specimens with r of 25% and 50%, respectively.

The SI_i and SI_s so determined are also presented in Table 3. In the calculations, $K_{ie,B}(K_{se,B})$ and $K_{ie,C}(K_{se,C})$ are the average value of two same specimens.

The results in Table 3 clearly show that, generally, RACFST columns with r of 25% and 50% generated slightly lower K_{ie} than conventional CFST columns by 1.5% to 6.9% and 2.7% to 8.3%, respectively. For the serviceability-level section flexural stiffness (K_{se}), the decreased ranges are 1.8% to 4.1% and 4.7% to 7.8%. Also, In terms of section flexural stiffness compared with the reference conventional CFST specimens, the behaviour of RACFST specimens is considered to be comparable, as only 1.5% to 8.3% and 1.8% to 7.8% initial section flexural stiffness and serviceability-level section flexural stiffness decreases are induced in RACFST specimens.

The lower initial and serviceability-level section flexural stiffness of RACFST may be caused by the lower elastic modulus of RAC compared with the reference conventional concrete, as the elastic modulus of RAC with r of 25% and 50% is 5.1% and 10.5% lower higher than that of the conventional concrete, respectively. This can be explained that large amount of old mortar with a relatively low modulus of elasticity is attached to original aggregate particles in recycled aggregates (Hansen 1992).

The influences of RCA replacement ratio (r) on the total dissipated energy (E) in each cycle also can be found in Fig. 12. It is shown that, at the same lateral deflection ratio (δ/δ_y), the RCA replacement ratio (r) has a moderate effect on the total dissipated energy under the same or similar axial load level. However, the total dissipated energy of RACFST specimens is appreciably higher than that of the reference conventional CFST specimens. This may be due to the fact that, under the same lateral force level, larger deformation is induced in RACFST columns compared with the conventional CFST columns (Han and Yang 2006a, 2006b).

The Effects of RCA replacement ratio (r) on the ductility index (DI) is also illustrated in Fig. 13. It can be found that, under the same or similar axial load level, DI values increase with the increase of RCA replacement ratio. This may be explained that, compared with the control conventional concrete, a better deformation ability was generated in RAC due to its lower elastic modulus.

3.4. Comparison of bearing capacities and flexural stiffness with predictions based on current design codes

The lateral bearing capacities of square RACFST columns predicted using the following six design methods are compared with the test results obtained in current tests, i.e.

- ACI (2005)
- AIJ (1997)
- AISC (2005)
- BS5400 (2005)
- DBJ13-51-2003 (2003) (The equations were listed in detail in Han *et al*. (2003)).
- Eurocode 4, Part 1 (2004)

In all design calculations, the improvement of the steel strength in the corner portion was not considered and the material partial safety factors were set to unity.

Comparisons of the tested lateral bearing capacities (P_{ue}) with predictions (P_{uc}) based on the code provisions are shown in Table 4.

Table 4 shows both the mean value and the standard deviation (COV) of P_{uc} / P_{ue} for the different design methods. Results in this table clearly indicate that all the methods are conservative. This implies that the bearing capacities of square RACFST beam-columns can be evaluated as being safe according to the formulae in above six design codes, regardless of RCA replacement ratio (r). The bearing capacities predicted by AISC and BS5400 are about 38% and 32% lower than those of the tests. The predictions of DBJ13-51-2003 show lower bearing capacities than those of the tests by about 20%. The bearing capacities predicted by ACI and AIJ are about 7% and 8% lower than those of the tests. Relatively, the proposed methods in EC4, achieving a mean value of 0.964 and COV of 0.054, provide the best prediction.

It should be noted that the current code provisions were not originally developed for recycled aggregate concrete (RAC) in-fill composite columns under constant axial load and cyclically increasing flexural loading. The purpose of the comparison is to evaluate their accuracy in predicting the bearing capacity of square RACFST beam-columns.

For the elastic section flexural stiffness (K), different equations are given in aforementioned six design codes, and can be uniformly expressed by the following formula:

$$K = a \cdot E_s \cdot I_s + b \cdot E_c \cdot I_c \tag{6}$$

where, the terms a and b are the constants in five codes except in AISC (2005); E_s and E_c are the modulus of elasticity of steel and concrete, respectively; I_s and I_c are moment of inertia for steel and

Table 4 Comparisons between predicted bearing capacities and test results

No.	Specimen label	P_{ue} (kN)	ACI (2005)		AIJ (1997)		AISC (2005)		BS5400 (2005)		DBJ13-51-2003 (2003)		EC4 (2004)	
			P_{uc} (kN)	$\frac{P_{uc}}{P_{ue}}$	P_{uc} (kN)	$\frac{P_{uc}}{P_{ue}}$	P_{uc} (kN)	$\frac{P_{uc}}{P_{ue}}$	P_{uc} (kN)	$\frac{P_{uc}}{P_{ue}}$	P_{uc} (kN)	$\frac{P_{uc}}{P_{ue}}$	P_{uc} (kN)	$\frac{P_{uc}}{P_{ue}}$
1	LB-1	106.9	111.5	1.043	98.8	0.924	85.5	0.8	100.9	0.944	101	0.945	108.7	1.017
2	LB-2	106.1	111.5	1.051	98.8	0.931	85.5	0.806	100.9	0.951	101	0.952	108.7	1.025
3	LC-1	105.3	108.9	1.034	97.9	0.93	85.5	0.812	99.8	0.948	97.4	0.925	107.2	1.018
4	LC-2	105.4	108.9	1.033	97.9	0.929	85.5	0.811	99.8	0.947	97.4	0.924	107.2	1.017
5	MB-1	122.8	116.5	0.949	120.9	0.985	75	0.611	79.1	0.644	105.7	0.861	118.7	0.967
6	MB-2	122.9	116.5	0.948	120.9	0.984	75	0.61	79.1	0.644	105.7	0.86	118.7	0.966
7	MC-1	119.3	112.2	0.94	116.5	0.977	74.5	0.624	78	0.654	100.7	0.844	115.9	0.972
8	MC-2	119.1	112.2	0.942	116.5	0.978	74.5	0.626	78	0.655	100.7	0.846	115.9	0.973
9	HB-1	129.8	106.9	0.824	114.6	0.883	57.7	0.445	59	0.455	83.6	0.644	122.2	0.941
10	HB-2	129.3	106.9	0.827	114.6	0.886	57.7	0.446	59	0.456	83.6	0.647	122.2	0.945
11	HC-1	127.6	97.3	0.763	103.1	0.808	53.6	0.42	54.4	0.426	73.8	0.578	110.4	0.865
12	HC-2	127.2	97.3	0.765	103.1	0.811	53.6	0.421	54.4	0.428	73.8	0.58	110.4	0.868
	Mean		0.927		0.919		0.619		0.679		0.8		0.964	
	COV		0.107		0.062		0.16		0.217		0.145		0.054	

concrete, respectively. Table 5 gives the values of a, b, E_s and E_c in six design codes, where f_c' is concrete compressive cylinder strength; w_c is the weight of concrete per unit volume ($1500 \le w_c \le 2500$ kg/m^3); $C_0 = A_s / (A_s + A_c)$, in which, A_s and A_c are the area of steel and concrete cross section (AISC 2005).

The predicted initial section flexural stiffness (K_{ic}) of RACFST columns based on the above code provisions are compared with the current experimental results (K_{ie}) in Table 6.

Table 6 illustrates both the mean value and the standard deviation (COV) of K_{ic} / K_{ie} for the different design methods. The results in Table 6 show that, AISC and EC4 give the initial section flexural stiffness about 15% and 9% higher than those of the tests, respectively. ACI, AIJ and BS5400 give the initial section flexural stiffness about 22%, 20% and 15% lower than those of the tests, respectively. The DBJ 13-51-2003 method gives a mean of 1.08 and a COV of 0.075, and is slightly higher than the test results.

The predicted serviceability-level section flexural stiffness (K_{sc}) of RACFST columns based on the code provisions are compared with the current experimental results (K_{se}) in Table 7.

Table 7 shows both the mean value and the standard deviation (COV) of K_{sc} / K_{se} for the different

Table 5 a, b, E_s and E_c values in different design methods

Factor	ACI (2005)	AIJ (1997)	AISC (2005)	BS5400 (2005)	DBJ13-51-2003 (2003)	EC4 (2004)
a	1	1	1	0.95	1	1
b	0.2	0.2	$(0.6+2C_0) \le 0.9$	0.45	0.6	0.6
E_s (N/mm^2)	200000	205800	200000	205000	206000	210000
E_c (N/mm^2)	$4700\sqrt{f_c'}$	$21000\sqrt{f_c'/19.6}$	$0.043 w_c^{1.5}\sqrt{f_c'}$	$450 f_{cu}$	$\frac{10^5}{2.2 + 34.7/f_{cu}}$	$22000 \cdot (f_c'/10)^{0.3}$

Table 6 Comparisons between predicted initial section flexural stiffness and test results

No.	Specimen label	K_{ie} (kN.m^2)	ACI (2005)		AIJ (1997)		AISC (2005)		BS5400 (2005)		DBJ13-51-2003 (2003)		EC4 (2004)	
			K_{ic} (kN.m^2)	$\frac{K_{ic}}{K_{ie}}$	K_{ic} (kN.m^2)	$\frac{K_{ic}}{K_{ie}}$	K_{ic} (kN.m^2)	$\frac{K_{ic}}{K_{ie}}$	K_{ic} (kN.m^2)	$\frac{K_{ic}}{K_{ie}}$	K_{ic} (kN.m^2)	$\frac{K_{ic}}{K_{ie}}$	K_{ic} (kN.m^2)	$\frac{K_{ic}}{K_{ie}}$
1	LB-1	1748	1487	0.851	1525	0.872	2218	1.269	1645	0.941	2059	1.178	2080	1.19
2	LB-2	1784	1487	0.834	1525	0.855	2218	1.243	1645	0.922	2059	1.154	2080	1.166
3	LC-1	1743	1469	0.843	1508	0.865	2148	1.232	1595	0.915	2038	1.169	2046	1.174
4	LC-2	1733	1469	0.848	1508	0.87	2148	1.239	1595	0.92	2038	1.176	2046	1.181
5	MB-1	1956	1487	0.76	1525	0.78	2218	1.134	1645	0.841	2059	1.053	2080	1.063
6	MB-2	1923	1487	0.773	1525	0.793	2218	1.153	1645	0.855	2059	1.071	2080	1.082
7	MC-1	1864	1469	0.788	1508	0.809	2148	1.152	1595	0.856	2038	1.093	2046	1.098
8	MC-2	1877	1469	0.783	1508	0.803	2148	1.144	1595	0.85	2038	1.086	2046	1.09
9	HB-1	2073	1487	0.717	1525	0.736	2218	1.07	1645	0.794	2059	0.993	2080	1.003
10	HB-2	2048	1487	0.726	1525	0.745	2218	1.083	1645	0.803	2059	1.005	2080	1.016
11	HC-1	2031	1469	0.723	1508	0.742	2148	1.058	1595	0.785	2038	1.003	2046	1.007
12	HC-2	2072	1469	0.709	1508	0.728	2148	1.037	1595	0.77	2038	0.984	2046	0.987
	Mean		0.78		0.8		1.151		0.854		1.08		1.088	
	COV		0.054		0.055		0.08		0.059		0.075		0.075	

Table 7 Comparisons between predicted serviceability-level section flexural stiffness and test results

No.	Specimen label	K_{se} (kN.m^2)	ACI (2005)		AIJ (1997)		AISC (2005)		BS5400 (2005)		DBJ13-51-2003 (2003)		EC4 (2004)	
			K_{sc} (kN.m^2)	$\frac{K_{sc}}{K_{se}}$	K_{sc} (kN.m^2)	$\frac{K_{sc}}{K_{se}}$	K_{sc} (kN.m^2)	$\frac{K_{sc}}{K_{se}}$	K_{sc} (kN.m^2)	$\frac{K_{sc}}{K_{se}}$	K_{sc} (kN.m^2)	$\frac{K_{sc}}{K_{se}}$	K_{sc} (kN.m^2)	$\frac{K_{sc}}{K_{se}}$
1	LB-1	1425	1487	1.044	1525	1.07	2218	1.556	1645	1.154	2059	1.445	2080	1.46
2	LB-2	1380	1487	1.078	1525	1.105	2218	1.607	1645	1.192	2059	1.492	2080	1.507
3	LC-1	1368	1469	1.074	1508	1.102	2148	1.57	1595	1.166	2038	1.49	2046	1.496
4	LC-2	1339	1469	1.097	1508	1.126	2148	1.604	1595	1.191	2038	1.522	2046	1.528
5	MB-1	1636	1487	0.909	1525	0.932	2218	1.356	1645	1.006	2059	1.259	2080	1.271
6	MB-2	1715	1487	0.867	1525	0.889	2218	1.293	1645	0.959	2059	1.201	2080	1.213
7	MC-1	1709	1469	0.86	1508	0.882	2148	1.257	1595	0.933	2038	1.193	2046	1.197
8	MC-2	1585	1469	0.927	1508	0.951	2148	1.355	1595	1.006	2038	1.286	2046	1.291
9	HB-1	1701	1487	0.874	1525	0.897	2218	1.304	1645	0.967	2059	1.21	2080	1.223
10	HB-2	1723	1487	0.863	1525	0.885	2218	1.287	1645	0.955	2059	1.195	2080	1.207
11	HC-1	1729	1469	0.85	1508	0.872	2148	1.242	1595	0.922	2038	1.179	2046	1.183
12	HC-2	1561	1469	0.941	1508	0.966	2148	1.376	1595	1.022	2038	1.306	2046	1.311
	Mean		0.949		0.973		1.401		1.039		1.315		1.324	
	COV		0.097		0.099		0.142		0.105		0.134		0.135	

design methods. The results in this table clearly indicate that, the serviceability-level section flexural stiffness predicted by AISC, DBJ 13-51-2003 and EC4 are about 40%, 32% and 32% higher than those of the tests, respectively. BS 5400 gives the serviceability-level section flexural stiffness about 4% higher than those of the tests. The serviceability-level section flexural stiffness predicted by ACI is about 5% lower than those of the tests. The AIJ method gives a mean of 0.973 and a COV of 0.099, the mean is just about 3% lower than the test results, is the beat means of prediction.

4. Analytical modeling

For comparison purposes, the theoretical model, which was developed for conventional square CFST columns under reversed cyclic flexural loading while subjected to constant axially compressive load (Han *et al*. 2003, Han 2007, Han *et al*. 2009), is temporarily employed in this paper for the prediction of the lateral force (P) versus mid-span lateral deflection (δ) hysteretic curves of RACFST beam-columns. In the calculations, the increase in the yielding strength of corner zone is considered based on the model suggested by Abdel-Rahman and Sivakumaran (1997).

The real length of column (1.5 m) is taken as the effective buckling length, because the measured deflection curves of the tested specimens are generally in the shape of a half-sine wave in two loading directions (as shown in Fig. 6).

Fig. 5 shows the comparisons of the $P-\delta$ hysteretic curves for all tested specimens between predicted and measured results; and the predicted results are found to exhibit satisfactory agreement with the test results. The predicted bearing capacities (P_{ua}) and the values of P_{ua}/P_{ue} are presented in Table 1. It can be seen that, in general, the predicted bearing capacities agree well with the measured results, and tend to safety. It also can be found from Fig. 5 that, for the specimens with higher axial load ratio (n) and

higher RCA replacement ratio (r), more obvious differences was caused between the predicted and measured results. This can be explained that, compared with the conventional concrete, the higher the RCA replacement ratio, the larger the amount of old mortar contained in RAC and the less compact the core concrete in RACFST. In this case, the steel tube of RACFST columns with higher axial load level is apt to local buckling. This is not considered in the theoretical model.

5. Conclusions

The experimental work in present paper is an endeavor to explore the possibility of using recycled aggregate concrete filled square steel tubular columns in practice in seismic zones. From the observed experimental behaviour and from the comparisons with predicted results, the following conclusions can be drawn:

(1) The typical failure modes of RACFST specimens under reversed cyclic flexural loading while subjected to constant axially compressive load are similar to those of the reference conventional CFST specimens.

(2) The RACFST specimens show slightly lower but comparable bearing capacity and section flexural stiffness over the control conventional CFST column.

(3) Compared with the test results, the predicted bearing capacities of the current design codes are conservative, and generally, the DBJ 13-51-2003 and AIJ method provide the best prediction of the initial and serviceability-level section flexural stiffness, respectively.

(4) In general, the theoretical model for conventional CFST members can be effectively utilized in predicting the seismic performance of RAC-filled steel SHS beam-columns.

(5) The experimental results show that square CFST columns with RAC made with up to 50% RCA by weight is suitable for structural use in seismic zones.

Acknowledgements

The research reported in the paper is supported by Start-Up Fund for Outstanding Incoming Researchers of Fujian Province, the Education Bureau fund of Fujian Province (JB05060), and the Science and Technology Fund of Fuzhou University (2004-XQ-19). The financial support is highly appreciated. The authors also express special thanks to Mr. Xin Wu for his assistance in the experiments. The authors are grateful to Professor Lin-Hai Han of Tsinghua University for his helpful discussions and advice.

Notation

B	Overall face width of square steel tube
CFST	Concrete filled steel tube
CI	Loss of capacity index
DI	Ductility index
E_c	Concrete modulus of elasticity
E_s	Steel modulus of elasticity

f_c'	Concrete compressive cylinder strength
f_{cu}	Concrete compressive cube strength
I_c	Moment of inertia for core concrete cross section
I_s	Moment of inertia for hollow steel cross section
K_{ic}	Predicted initial section flexural stiffness
K_{ie}	Experimental initial section flexural stiffness
K_{sc}	Predicted serviceability-level section flexural stiffness
K_{se}	Experimental serviceability-level section flexural stiffness
L	Effective buckling length of column in the plane of bending
M	Moment
M_{ue}	Experimental ultimate moment
n	Axial load level (= N_o / N_u)
NCA	Natural coarse aggregate
N_o	Applied axially compressive load
N_u	Axially compressive capacity
P	Lateral force
P_{uc}	Predicted bearing capacity
P_{ue}	Experimental bearing capacity
r	Recycled coarse aggregate replacement ratio
RAC	Recycled aggregate concrete
RACFST	Recycled aggregate concrete filled steel tube
RCA	Recycled coarse aggregate
SI_i	Loss of initial section flexural stiffness index
SI_s	Loss of serviceability-level section flexural stiffness index
t	Wall thickness of steel tube
δ	Mid-span lateral deflection
δ_y	Yield lateral deflection
δ_u	Lateral deflection when the lateral force falls to 85% of the bearing capacity
ϕ	Curvature

References

Abdel-Rahman, N. and Sivakumaran, K.S. (1997), "Material properties models for analysis of cold-formed steel members", *J. Struct. Eng. ASCE*, **123**(9), 1135-1143.

ACI 318-05 (2005), *Building code requirements for structural concrete and commentary*, Farmington Hills (MI), American Concrete Institute, Detroit, U.S.A.

AIJ (1997), *Recommendations for design and construction of concrete filled steel tubular structures*, Architectural Institute of Japan, Tokyo, Japan.

Ajdukiewicz, A. and Kliszczewicz, A. (2002), "Influences of recycled aggregates on mechanical properties of HS/HPC", *Cement Concrete Comp.*, **24**(2), 269-279.

ANSI/AISC 360-05 (2005), *Specification for structural steel buildings*, American Institute of Steel Construction

(AISC), Chicago, U.S.A.
ATC-24 (1992), *Guidelines for cyclic seismic testing of components of steel structures*, Applied Technology Council, Redwood City (CA), U.S.A.
BS5400-5 (2005), *Steel, concrete and composite bridges, Part 5: Code of practice for the design of composite bridges*, British Standard Institute, London, UK.
DBJ 13-51-2003 (2003), *Technical specification for concrete-filled steel tubular structures*, Fuzhou (in Chinese).
Etxeberria, M., Marí, A.R. and Vázquez, E. (2007), "Recycled aggregate concrete as structural material", *Mater. Struct.*, **40**, 529-541.
Eurocode 4 (2004), *Design of steel and concrete structures, Part1-1: General rules and rules for building*, EN 1994-1-1: 2004, European Committee for Standardization, Brussels.
Evangelista, L. and de Brito, J. (2007), "Mechanical behaviour of concrete made with fine recycled concrete aggregates", *Cements Concrete comp.*, **29**, 397-401.
Han, L.H. (2007), *Concrete-Filled Steel Tubular Structures-Theory and Practice (Second edition)*, China Science Press, Beijing (in Chinese).
Han, L.H., Huang, H., Tao, Z. and Zhao, X.L. (2006), "Concrete-filled double skin steel tubular (CFDST) beam-columns subjected to cyclic bending", *Eng. Struct.*, **28**(12), 1698-1714.
Han, L. H., Huang, H. and Zhao, X. L. (2009), "Analytical Behaviour of Concrete-Filled Double Skin Steel Tubular (CFDST) Beam-Columns under Cyclic loading," *Thin Wall. Struct.* (Articles in Press).
Han, L.H., Yang, Y.F. (2005), "Cyclic performance of concrete-filled steel CHS columns under flexural loading", *J. Constr. Steel Res.*, **61**(4), 423-452.
Han, L.H., Yang, Y.F. and Tao, Z. (2003), "Concrete-filled thin walled steel RHS beam-columns subjected to cyclic loading", *Thin wall. Struct.*, **41**(9), 801-833.
Han, L.H., Yao, G.H., Chen, Z.B. and Yu, Q. (2005a), "Experimental behaviors of steel tube confined concrete (STCC) columns", *Steel Compos. Struct.*, **5**(6), 459-484.
Han, L.H., You, J.T. and Lin, X.K. (2005b), "Experimental behaviour of self-consolidating concrete (SCC) filled hollow structural steel (HSS) columns subjected to cyclic loading", *Adv. Struct. Eng.*, **8**(5), 497-512.
Hansen, T.C. (1992), *Recycling of Demolished Concrete and Masonry*, In: Hansen TC (Ed.), Report of RILEM TC 37-DRC on Demolition and Reuse of Concrete, E&FN Spon, London, UK.
Poon, C. and Chan, D. (2007), "The use of recycled aggregate in concrete in Hong Kong", *Resour. Conserv. Recy.*, **50**, 293-305.
Rao, A., Jha, K. N. and Misra, S. (2007), "Use of aggregates from recycled construction and demolition waste in concrete", *Resour. Conserv. Recy.*, **50**, 71-81.
Varma, A.H., Ricles, J.M., Sause, R. and Lu, L.W. (2002), "Seismic behavior and modeling of high-strength composite concrete-filled steel tube (CFT) beam-columns", *J. Constr. Steel Res.*, **58**(5-8), 725-758.
Yang, Y.F. and Han, L.H. (2006a), "Compressive and flexural behaviour of recycled aggregate concrete filled steel tubes (RACFST) under short-term loadings", *Steel Compos. Struct.*, **7**(3), 257-284.
Yang, Y.F. and Han, L.H. (2006b), "Experimental behaviour of recycled aggregate concrete filled steel tubular columns", *J. Constr. Steel Res.*, **62**(12), 1310-1324.
Yang, Y.F., Han, L.H. and Zhu, L.T. (2008), "Experimental performance of recycled aggregate concrete-filled circular steel tubular columns subjected to cyclic flexural loadings", *Adv. Struct. Eng*. (Accepted).
Zega, C.J. and Di Maio, A.A. (2006), "Recycled concrete exposed to high temperatures", Mag. Concrete Res., **58**(10), 675-682.

CC